SDF-1/CXCR4 induces epithelial-mesenchymal transition through activation of the Wnt/β-catenin signaling pathway in rat chronic allograft nephropathy

HAO TANG[*], YUE XU[*], ZIJIAN ZHANG, SONG ZENG, WENBO DONG, WENJIAO JIAO and XIAOPENG HU

Urology Institute of Capital Medical University, Department of Urology,
Capital Medical University Beijing Chaoyang Hospital, Beijing 100020, P.R. China

Abstract. Epithelial-mesenchymal transition (EMT) has been demonstrated to serve a crucial role in the progression of interstitial fibrosis, which is one of the principal pathological features of chronic allograft nephropathy (CAN). However, to the best of our knowledge, the mechanisms of EMT in CAN have not been investigated. In the present study, the effect of stromal cell-derived factor 1 (SDF-1) and the Wnt signaling pathway on the progression of EMT following kidney transplantation was investigated. The CAN model was established using Fisher 344 and Lewis rats, treated with low-dose cyclosporine with or without AMD3100. CAN was confirmed by the pathological alterations and chronic allograft damage index scoring, and EMT was confirmed by western blotting and reverse transcription-quantitative polymerase chain reaction. In the AMD3100 group, there were lower expression levels of α-SMA and higher expression levels of E-cadherin, which indicated that CAN and EMT were ameliorated by AMD3100. The kidney tissue was analyzed using an mRNA + long noncoding (lnc)RNA microarray. A total of 506 mRNAs and 404 lncRNAs were demonstrated to be significantly differentially expressed between the two groups, which revealed the involvement of SDF-1/CXC chemokine receptor 4 (CXCR4) and the Wnt pathway. SDF-1 was demonstrated to induce EMT *in vitro* through the upregulation of α-SMA, downregulation of E-cadherin and the wound healing assay, and in the rat renal tubular epithelial cells via the nuclear accumulation of β-catenin, which were all inhibited by either AMD3100 or DKK-1. CXXC finger protein 5 (CXXC5), a negative regulator of the Wnt pathway, was downregulated following treatment with SDF-1, which was inhibited by AMD3100 but not by DKK-1. Thus, CXXC5 may be a regulator downstream of SDF-1/CXCR4 in EMT. In conclusion, SDF-1/CXCR4 induces EMT of renal tubular epithelial cells with the involvement of the Wnt pathway, which may be a novel mechanism and therapeutic target in kidney allograft fibrosis of rats.

Introduction

Kidney transplantation is the only effective treatment for end-stage renal disease and the 10-year survival rate following allografts is <50% (1,2). Interstitial fibrosis and tubular atrophy are the principal pathological features of chronic allograft nephropathy (CAN), which is the primary cause of late renal allograft loss (3,4). Epithelial-mesenchymal transition (EMT) has been demonstrated to serve a crucial role in the process of interstitial fibrosis (5).

CXC chemokine receptor 4 (CXCR4), the receptor of stromal cell-derived factor 1 (SDF-1), has been demonstrated to be expressed at lower levels in normal human kidneys (6), and the expression levels were increased in a mouse model of renal ischemia (7). Activation of the SDF-1/CXCR4 pathway has been demonstrated to contribute to the progression of CAN, and inhibition of CXCR4 by AMD3100 attenuates the progression of renal allograft fibrosis (8). Blockade of SDF-1/CXCR4 by AMD3100 has been reported to serve a protective role following kidney transplantation by mobilizing stem cells (9-11), but the mechanism in allografts has not been studied to the best of our knowledge. Studies have demonstrated that SDF-1 is able to induce EMT and tissue fibrosis (7,12,13), including kidney fibrosis (14,15). The Wnt signaling pathway has been reported to be involved in the initiation and progression of chronic renal allograft damage in a rat model (16). Previous studies have also reported that the Wnt/β-catenin pathway serves an important role in SDF-1-induced EMT in numerous types of tumors (17,18). However, there are few studies that have focused on the mechanisms of EMT in tubular epithelial cells following kidney transplantation. To the best of our knowledge, the present study is the first to

Correspondence to: Professor Xiaopeng Hu, Urology Institute of Capital Medical University, Department of Urology, Capital Medical University Beijing Chaoyang Hospital, 8 Gong Ti Nan Lu, Beijing 100020, P.R. China
E-mail: xiaopeng_hu@sina.com

[*]Contributed equally

investigate the mechanisms of SDF-1 and the Wnt pathway in kidney allograft fibrosis.

In the present study, EMT was demonstrated to be ameliorated by AMD3100 in the rat CAN model. Variations in markers and RNAs in the rat CAN model were analyzed and the results revealed the association between SDF-1/CXCR4 and the Wnt pathway. Subsequently, the involvement of the Wnt signaling pathway in SDF-1-induced renal tubular EMT was investigated *in vitro*, which may be a novel mechanism of renal allograft fibrosis.

Materials and methods

Animal models. The experimental animals included 10 male Fisher (F344) rats as the donors and 10 male Lewis (LEW) rats as the recipients. All animals were aged between 8-12 weeks and weighed 200-250 g. Animals were provided by Beijing Vital River Laboratory Animal Technology Co., Ltd. (Beijing, China). The F344-LEW rat CAN model was established as previously described (8). The rats were divided randomly into the following two groups: The AMD3100 group and the CAN group. The rats in the AMD3100 group were administered subcutaneous injections of low-dose cyclosporine (1.5 mg/kg) every day in the first 10 days post-transplantation and AMD3100 (Sigma-Aldrich; Merck KGaA, Darmstadt, Germany; 1 mg/kg) at 0, 2, 4, 6, 8 and 10 days post-transplantation, and the rats in the CAN group were administered subcutaneous injections of low-dose cyclosporine (1.5 mg/kg/day) and saline at a dose equivalent to AMD3100 in the first 10 days following transplantation. At 12 weeks post-surgery, the kidney allografts in both the AMD3100 and CAN groups were harvested under anesthesia using 2% pentobarbital sodium (40 mg/kg), and the rats were subsequently administered pentobarbital sodium (200 mg/kg). The animals were protected by following the National Institutes of Health Guide for the Care and Use of Laboratory Animals (19). The animal protocols were approved by the Medical Research Center, Beijing Chaoyang Hospital, Capital Medical University (Beijing, China). The housing conditions were as follows: Temperature, 22±1°C; relative humidity, 55±5% and free access to water and normal diet under an alternating 12:12-h light-dark cycle.

Histopathology and immunohistochemistry. The kidneys were cut longitudinally along the coronal plane and fixed in 10% neutral formalin solution at room temperature for 24 h, followed by dehydration with alcohol, embedding in paraffin, and sectioning into 2-μm thick slices. Hematoxylin and eosin, and Masson's trichrome staining were performed to assess the renal injury. For hematoxylin and eosin staining, the sections were stained at room temperature with hematoxylin for 5 min and eosin for 2 min. For Masson's trichrome staining (all steps conducted at room temperature), the nuclei were stained with Weigert's iron hematoxylin for 10 min, followed by plasma membrane staining with acid fuchsin, Xylidine Ponceau, and glacial acetic acid for 10 min, phosphomolybdic acid staining for 5 min, and fiber staining with methyl blue for 10 min. A total of two experienced pathologists independently evaluated the results of the histopathological analysis, and the images were acquired at x400 magnification. The chronic allograft damage index (CADI) scores of the kidney specimens in

the two groups were determined. The CADI scoring system covers the following six pathological aspects of CAN: Renal interstitial inflammation, interstitial fibrosis, tubular atrophy, basement membrane matrix thickening, glomerular sclerosis and arterial intimal hyperplasia (20).

Immunohistochemistry was performed using the same procedures of dehydration, embedding and sectioning. Endogenous peroxidase was blocked with 3% H_2O_2 at room temperature for 10 min, and then the specimens were heated in a citrate buffer (pH 6.0) to 98°C for 15 min. The primary goat anti-CXCR4 antibody (cat. no. ab1670; Abcam, Cambridge, UK; 1:1,000) was added in a dropwise manner to the sections, which were incubated at 4°C overnight. Subsequently, the specimens were incubated with horseradish peroxidase (HRP)-conjugated donkey anti-goat immunoglobulin G (cat. no. A0181; Beyotime Institute of Biotechnology, Haimen, China; 1:50) at 37°C for 30 min. A freshly prepared 0.05% 3,3'-diaminobenzidine solution was added to each specimen section. The color reaction was observed and controlled by light microscopy (Olympus Corporation, Tokyo, Japan), and terminated by washing with tap water. Images were acquired at x400 magnification.

Microarrays and pathway analysis. Total RNA was extracted from the kidney tissues using TRIzol® (Invitrogen; Thermo Fisher Scientific, Inc., Waltham, MA, USA) reagent, and the purity and concentration of the RNA was determined from the $OD_{260/280}$ readings of a spectrophotometer. The RNA integrity was determined by capillary electrophoresis using the RNA 6000 Nano Lab-on-a-Chip kit and a Bioanalyzer 2100 (both Agilent Technologies, Inc., Santa Clara, CA, USA). Only RNA extracts with RNA integrity values of >6 were subjected to further analysis. Higher yields of cDNA were labeled with a fluorescent dye (Cy5 and Cy3-dCTP) using the CapitalBio cRNA Amplification and Labeling kit (CapitalBio, Beijing, China). The labeled cRNAs from long noncoding (lnc)RNAs and mRNAs were purified and hybridized to the Agilent Rat lncRNA + mRNA Array V1.0 (Agilent Technologies, Inc.). Images were captured by the Agilent microarray scanner, gridded and then analyzed using Agilent Feature Extraction software, version 10.10 (Agilent Technologies, Inc.). The raw data were summarized and normalized using GeneSpring software V12.0 (Agilent Technologies, Inc.).

The threshold values of ≥2 absolute fold change (FC) and a Benjamini-Hochberg corrected P-value of ≤0.05 were used. The data were log2 transformed and median-centered using the Adjust Data function of Cluster 3.0 software (http://bonsai.hgc.jp/~mdehoon/software/cluster/index.html). These genes were classified according to the Gene Ontology (GO) analysis provided by the Molecular Annotation System 3.0 (http://bioinfo.capitalbio.com/mas3/). Signaling pathway analysis of these genes was performed with the Kyoto Encyclopedia of Genes and Genomes (KEGG) pathway database (http://www.kegg.jp/kegg/pathway.html).

Cell culture. The rat renal tubular epithelial cell line NRK-52E was purchased from American Type Culture Collection (Manassas, VA, USA) and cultured in Dulbecco's modified Eagle's medium (DMEM) containing 10% fetal bovine serum (Gibco; Thermo Fisher Scientific, Inc.) and 1%

Table I. Primers for reverse transcription-quantitative polymerase chain reaction.

Target gene	Primer name	Oligonucleotide sequence (5'-3')
GAPDH	GAPDH-F	GGCAAGTTCAACGGCACAG
	GAPDH-R	CGCCAGTAGACTCCACGACAT
α-SMA	α-SMA-F	AGCTGCTCCAGCTATGTGTG
	α-SMA-R	TCCCAGTTGGTGATGATGCC
E-cadherin	E-cadherin-F	GTGCCACCACCAAAGATA
	E-cadherin-R	GGCTGAGACAACCCTAAT
CXXC5	CXXC5-F	GCAGTGCAGCAGTTGTAGGA
	CXXC5-R	GACGGAAGCATCACCTTCTC
LOC100912353	LOC100912353-F	CGGGAACCTAGGAATGACAA
	LOC100912353-R	CAACGTTCTTGGTCCTCCAT
LOC102551030	LOC102551030-F	AAGCCGGTGTGAAGATCAAC
	LOC102551030-R	TCCTCGGGAATCACAGAAAC
LOC102556393	LOC102556393-F	ATGTAGGTTTGCCCAAGCAC
	LOC102556393-R	AACTGCAGGACAGGCATCTAA

F, forward; R, reverse; α-SMA, α-smooth muscle actin; CXXC5, CXXC finger protein 5.

penicillin/streptomycin (Lablead Biotech Co., Ltd., Beijing, China) at 37°C with 5% CO_2. The NRK-52E cells with optimal morphology were digested and seeded in a 60-mm dish at a concentration of ~$1x10^5$ cells/dish.

Treatment in vitro. Once the cells had attached, the medium was changed to DMEM without serum. After 24 h, the cells were divided into four groups and treated as follows: SDF-1 group, 100 ng/ml SDF-1 (cat. no. ab79959; Abcam); SDF-1 + AMD3100 group, 100 ng/ml SDF-1 and 5 μg/ml AMD3100 (Sigma-Aldrich; Merck KGaA); SDF-1 + DKK-1 group, 100 ng/ml SDF-1 and 200 ng/ml DKK-1 (R&D Systems, Inc., Minneapolis, MN, USA); and control group, PBS at a dose equivalent to the SDF-1, AMD3100 and DKK-1 in the other groups.

Following incubation at 37°C for 24 h, the cellular total protein and nuclear protein were extracted for western blotting (WB) and the total RNA was extracted for reverse transcription-quantitative polymerase chain reaction (RT-qPCR).

WB. The cells were divided into two groups; one group was lysed in radioimmunoprecipitation assay lysis buffer (Beyotime Institute of Biotechnology) containing phenylmethylsulfonyl fluoride and the other group was lysed using a Nuclear and Cytoplasmic Protein Extraction kit (Beyotime Institute of Biotechnology). The lysed cells were centrifuged at 14,000 x g for 20 min at 4°C. The protein concentration was measured using a bicinchoninic acid assay kit (Beyotime Institute of Biotechnology). The proteins were mixed with loading buffer and boiled for 10 min, and subjected to 10% SDS-PAGE, with 30 μg protein loaded per lane. The separated proteins were transferred to polyvinylidene fluoride membranes (EMD Millipore, Billerica, MA, USA). Following blocking of the nonspecific background in 5% milk at room temperature for 1 h, the membranes were incubated overnight at 4°C with the following

primary antibodies: Rabbit anti-α-tubulin (cat. no. 2125; Cell Signaling Technology, Inc., Danvers, MA, USA; 1:2,000); rabbit anti-α-SMA (cat. no. ab5694; Abcam; 1:4,000); mouse anti-E-cadherin (cat. no. 14472; Cell Signaling Technology, Inc.; 1:1,000); rabbit anti-CXCR4 (cat. no. ab124824; Abcam; 1:2,000); rabbit anti-lamin B1 (cat. no. 13435; Cell Signaling Technology, Inc.; 1:1,000); rabbit anti-CXXC finger protein 5 (CXXC5; cat. no. 84546; Cell Signaling Technology, Inc.; 1:1,000) and rabbit anti-β-catenin (cat. no. 8480; Cell Signaling Technology, Inc.; 1:1,000). Subsequently, the membranes were washed with TBS with Tween-20 and incubated with the HRP-conjugated secondary antibodies (cat. no. TA130003 and cat. no. TA140003; OriGene Technologies, Inc., Beijing, China; 1:1,000) at room temperature for 1 h. Immobilon Western Chemiluminescent Horseradish Peroxidase Substrate (EMD Millipore) was used to detect positive immune reactions. α-Tubulin was used as the reference for total protein and lamin B1 was used as the reference for nuclear protein. Densitometric analysis was performed using Image Lab 3.0 (Bio-Rad Laboratories, Inc., Hercules, CA, USA).

RT-qPCR. Total RNA was extracted from the cells using TRIzol® reagent and reverse-transcribed into cDNA using a SuperScript IV First-Strand Synthesis System (Invitrogen; Thermo Fisher Scientific, Inc.) following the manufacturer's protocols. The RT-qPCR reactions were performed on the ABI 7500 Real-Time PCR System (Applied Biosystems; Thermo Fisher Scientific, Inc.) using a SuperScript III Platinum SYBR Green One-Step RT-qPCR Kit (Invitrogen; Thermo Fisher Scientific, Inc.); the primers used are listed in Table I. The target mRNA levels were normalized against GAPDH mRNA standards and calculated using the $2^{-\Delta\Delta Cq}$ method (21).

Wound healing assay. The NRK-52E cells were cultured under standard conditions to 80-90% confluence, and were pretreated
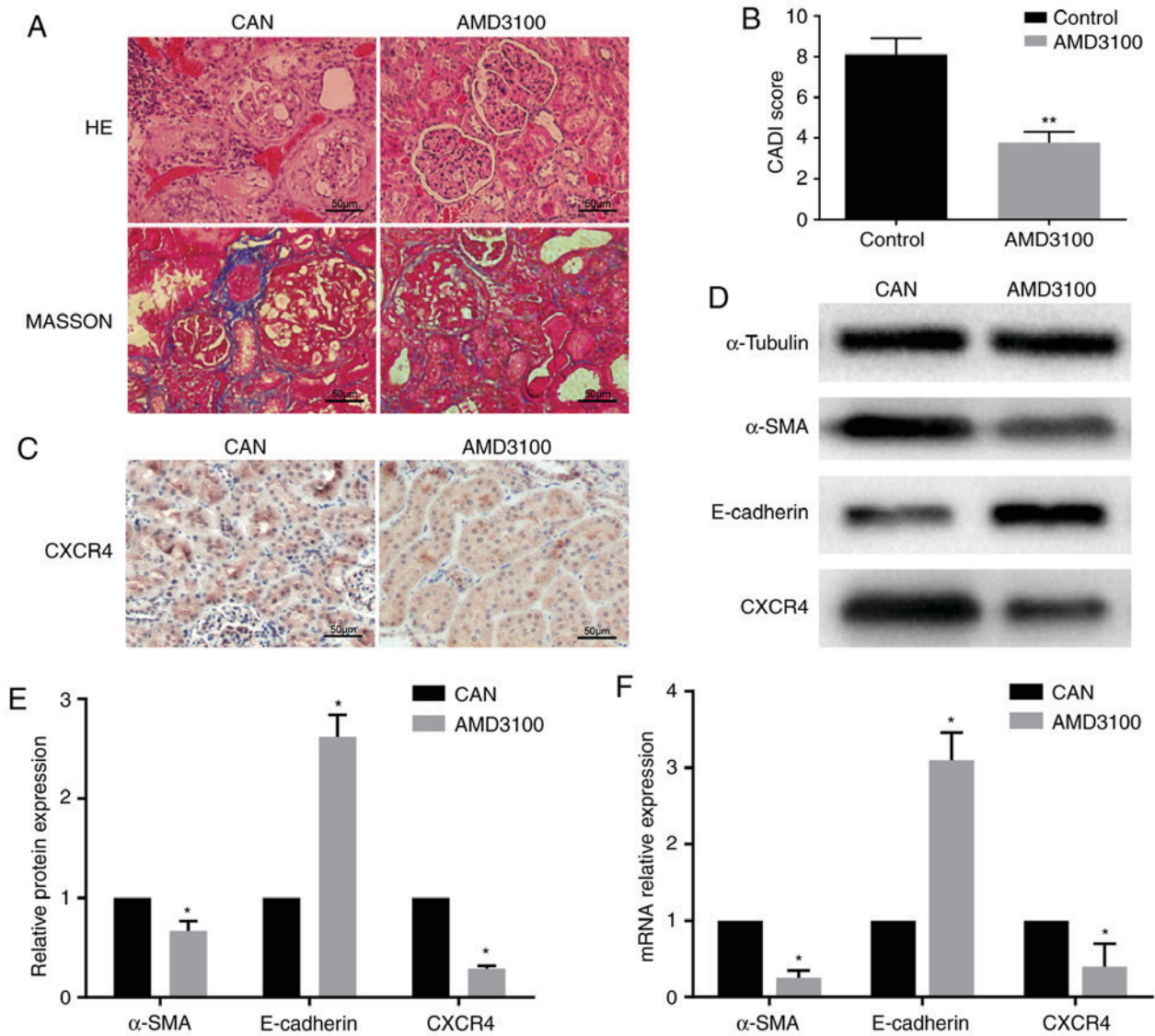
Figure 1. Fibrosis and epithelial-mesenchymal transition in rat kidney allografts. (A) HE and Masson's trichrome staining revealed that the AMD3100 group exhibited milder interstitial fibrosis compared with the CAN group. (B) The AMD3100 group had a lower CADI score compared with the CAN group. **P<0.01 vs. control. (C) Immunohistochemistry revealed the expression of CXCR4 in the tubules, and it was expressed at a lower level in the AMD3100 group. (D) WB demonstrated the downregulation of α-SMA and CXCR4 and the upregulation of E-cadherin in the AMD3100 group. (E) Grayscale analysis of the WB. (F) RT-qPCR revealed that α-SMA and CXCR4 mRNA were downregulated and E-cadherin mRNA was upregulated in the AMD3100 group. *P<0.05 vs. respective CAN group. CAN, chronic allograft nephropathy; CADI, chronic allograft damage index; CXCR4, CXC chemokine receptor 4; WB, western blotting; HE, hematoxylin and eosin; α-SMA, α-smooth muscle actin.

with DMEM without serum at 37˚C for 24 h. Subsequently, the cells were treated with 100 mg/ml SDF-1 with or without 5 µg/ml AMD3100 and 200 ng/ml DKK-1 during the wound healing assay. Cell migration was assessed by measuring the movement of cells into the acellular area created by a sterile insert at 0, 12 and 24 h following scratching (magnification, x400).

Statistical analysis. Statistical analysis and data processing were performed using SPSS version 20 (IBM Corp., Armonk, NY, USA). The normally distributed measurement data are expressed as the mean ± standrd deviation of experiments that were replicated three times. The independent samples t-test was used to compare two groups when the data were normally distributed and exhibited homogeneity of variance. Comparison between multiple groups was conducted

using one-way analysis of variance followed by a least significance difference test. If the data exhibited a skewed distribution or failed to present homogeneity of variance, the Mann-Whitney U test was used for the comparison of two groups. P<0.05 was considered to indicate a statistically significant difference.

Results

SDF-1/CXCR4 axis in the rat CAN model. The histopathological changes and CADI scores confirmed CAN in the rat kidney grafts at 12 weeks post-transplantation. The AMD3100 group exhibited milder tubular atrophy, inflammatory cell infiltration and interstitial fibrosis, and also had a lower CADI score compared with the CAN group (Fig. 1A and B). Subsequently, the expression levels of a number of fibrosis-associated
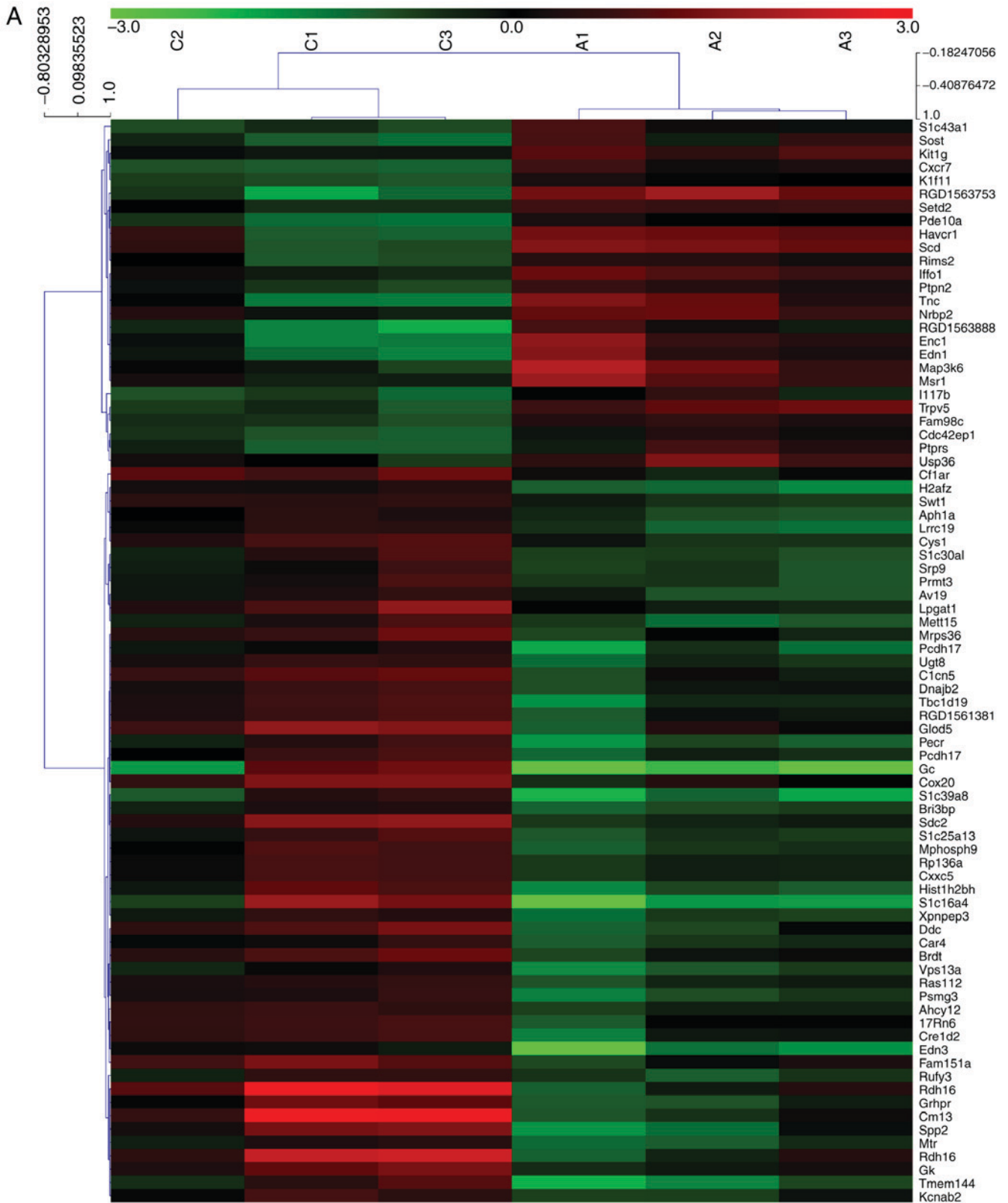
Figure 2. mRNA + lncRNA microarray analysis of kidney allograft tissues. (A) Clustering analysis of the mRNAs revealed that 81 mRNAs were significantly differentially expressed (FC>2.0; P<0.05) between the CAN group (C1-3) and the AMD3100 group (A1-3).

markers were detected. Using immunohistochemistry, CXCR4 was observed in the tubules in the CAN group, but it was expressed at lower levels in the AMD3100 group (Fig. 1C). RT-qPCR demonstrated that the expression of α-SMA was downregulated and that of E-cadherin was upregulated in the

AMD3100 group compared with the CAN group, which was confirmed at the protein level by WB (Fig. 1D-F). The expression of CXCR4 was downregulated following administration of AMD3100 (Fig. 1D and F). These findings indicated the protective effect of AMD3100 in rat CAN by inhibiting the
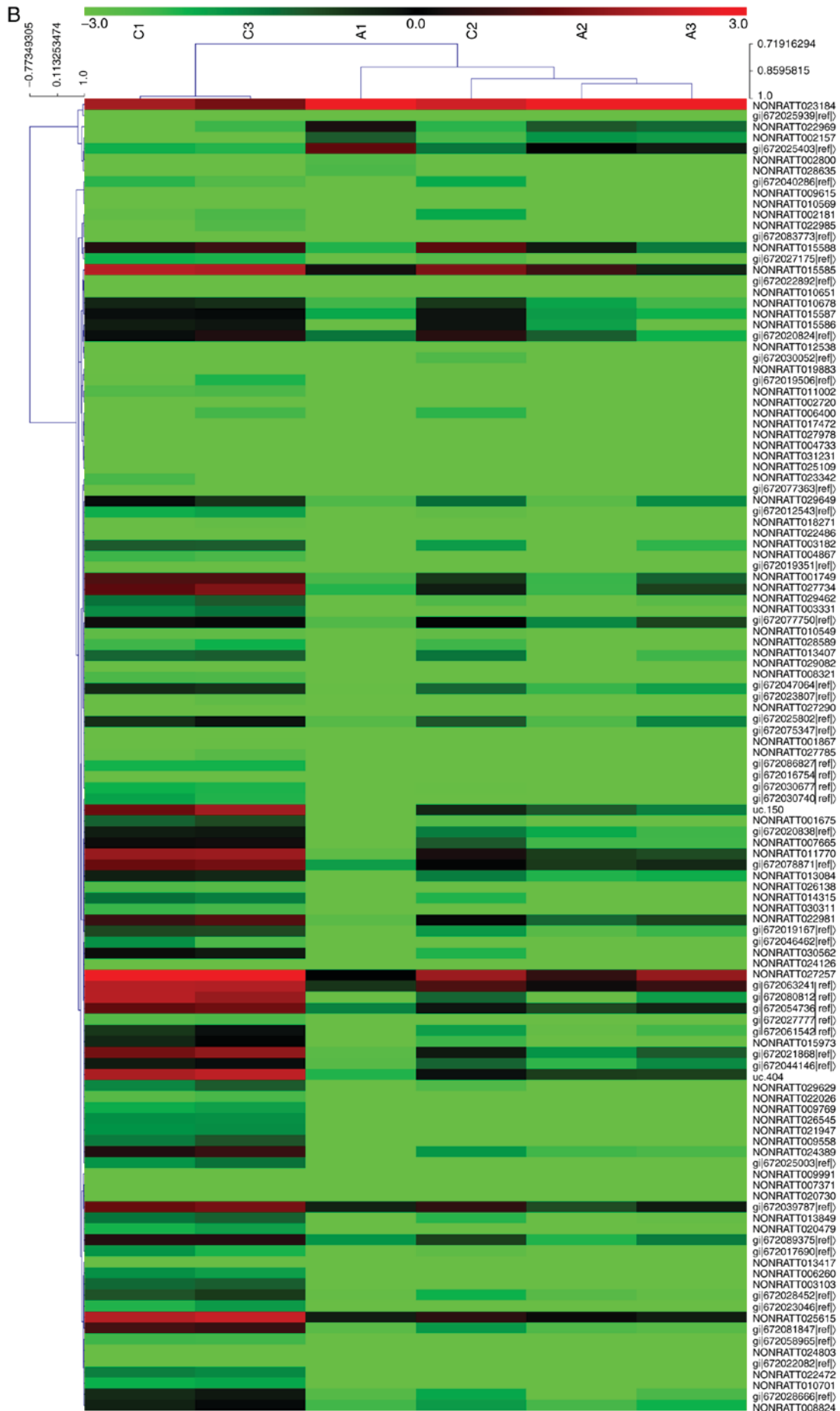
Figure 2. Continued. mRNA + lncRNA microarray analysis of kidney allograft tissues. (B) Cluster analysis of lncRNAs demonstrated that 140 lncRNAs were significantly differentially expressed (FC>2.0; P<0.05) between the two groups.
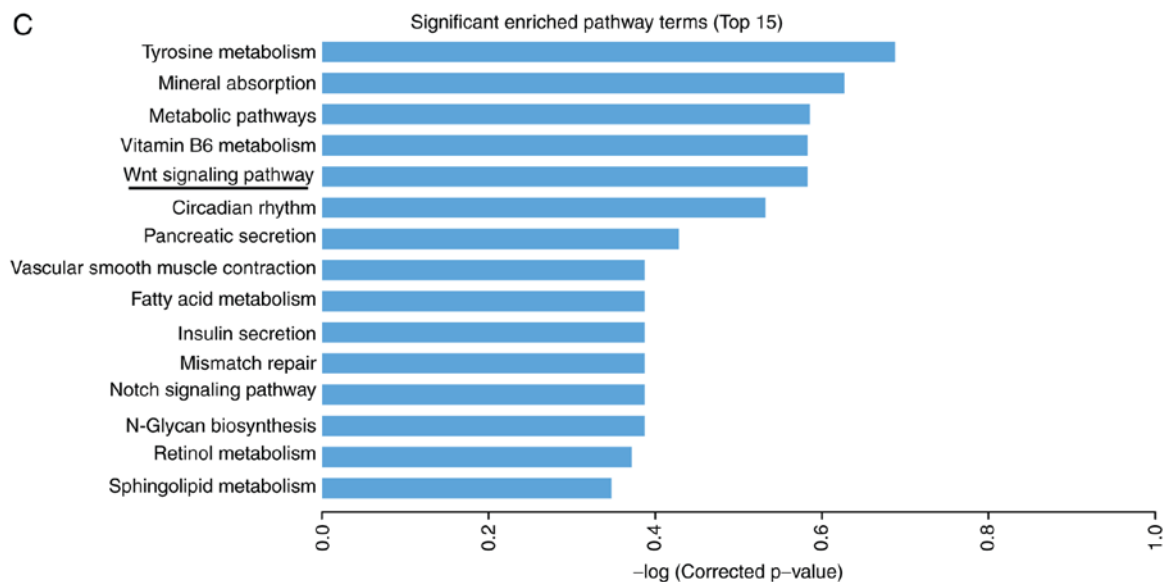
Figure 2. Continued. mRNA + lncRNA microarray analysis of kidney allograft tissues. (C) The top 15 pathways suggested by the Kyoto Encyclopedia of Genes and Genomes pathway analysis. FC, fold change; CAN, chronic allograft nephropathy; lncRNA, long noncoding RNA.

SDF-1/CXCR4 axis, and the SDF-1/CXCR4 axis may serve an important role in CAN.

Microarray and pathway analysis. In order to analyze alterations in the expression of mRNAs and lncRNAs in the rat CAN model, the kidney allograft tissues of the AMD3100 group and the CAN group were analyzed using an mRNA + lncRNA microarray. The results of the microarray were uploaded to the Gene Expression Omnibus database (GSE114088). Clustering analysis revealed that 506 mRNAs and 404 lncRNAs were significantly differentially expressed between the two groups, including 81 mRNAs and 140 lncRNAs with an FC value >2.0 (Fig. 2A and B). KEGG pathway analysis revealed that one of the top ranked pathways was the Wnt signaling pathway (Fig. 2C), which has been widely reported to be an important mechanism in EMT and fibrosis (22,23). The results of the microarray also predicted the association of a number of lncRNAs and mRNAs. CXXC5 mRNA was demonstrated to be negatively correlated with the lncRNAs LOC100912353, LOC102551030 and LOC102556393, which, it may be considered, may be a probable target for regulating renal allograft fibrosis (Table II). The coding potential of these lncRNAs is low, with the PhyloCSF (24) scores <-100 (Table II).

EMT is induced by SDF-1 and inhibited by AMD3100 and DKK-1 in vitro. Variation in the expression levels of EMT-associated markers in the different groups of NRK-52E cells was quantitated using RT-qPCR and WB. In the SDF-1 group, α-SMA was upregulated and E-cadherin was significantly downregulated (P<0.05) compared with the other groups (Fig. 3A-C). These results confirmed that EMT was induced by SDF-1 in renal tubular epithelial cells, and this was antagonized by AMD3100 and DKK-1.

Wound healing assay. The results of the wound healing assay revealed that SDF-1 promoted cell migration across the wound edge into the scratch area at 12 and 24 h compared

with the other groups. In the SDF-1 + AMD3100 group and SDF-1 + DKK-1 group, extensive cell migration was not observed until 24 h post-treatment (Fig. 3D and E).

Markers of the Wnt/β-catenin pathway. The protein expression levels of β-catenin in the nucleus were increased significantly in the SDF-1 group, while the increase in the levels of total β-catenin was not as significant (Fig. 4), indicating the nuclear accumulation of β-catenin. The WB and RT-qPCR results demonstrated a reduction in the levels of CXXC5 expression in the SDF-1 group compared with the control group; however, expression in the SDF-1 + AMD3100 group was not significantly different to that in the control group. Notably, CXXC5 was also downregulated in the SDF-1 + DKK-1 group (Fig. 4A-C). These results suggested that CXXC5 is involved in EMT induced by the SDF-1/CXCR4 axis, and CXXC5 may be a potential upstream regulator of the WNT/β-catenin pathway.

Involvement of lncRNAs. In order to detect the expression of the aforementioned lncRNAs, RT-qPCR was performed. Two of these lncRNAs were demonstrated to be significantly upregulated in the SDF-1 group and the SDF-1 + DKK-1 group, but not the SDF-1 + AMD3100 group, compared with the control group (Fig. 4D).

Discussion

The SDF-1/CXCR4 axis serves crucial roles in promoting proliferation and metastasis (25). A previous study reported the protective effect of AMD3100 in kidney injuries (26). A number of studies have demonstrated that inhibition of the SDF-1/CXCR4 axis with AMD3100 leads to prolonged allograft survival, which is due to an influx of host stem cells that results in a modulated host immune response (9,10). A previous study revealed that the progression of allograft fibrosis in a rat CAN model is attenuated by AMD3100 (8).

Table II. Relevant lncRNAs.

lncRNA gene name	Chromosome	Strand	Start	End	GI	Length (bp)	NCBI RefSeq	NONCODE	PhyloCSF
LOC100912353	3	+	1732192	1733260	672046462	718	XR_145884.3	NONRATT018415	-115.53
LOC102551030	2	+	3404984	3412416	672042805	3190	XR_591163.1	-	-999.16
LOC102556393	X	+	4623698	4626807	672087756	1937	XR_597614.1	-	-580.58

lncRNA, long noncoding RNA; NCBI, National Center for Biotechnology Information.

However, the effect and mechanisms of SDF-1/CXCR4 on fibrosis in renal allografts have rarely been reported.

In the present study, rats were treated with AMD3100 and it was demonstrated that the blockade of SDF-1/CXCR4 may mediate the development of CAN. The results of the mRNA + lncRNA microarray revealed that activation of the Wnt pathway may serve an important role in the fibrosis of the CAN model. The *in vitro* results demonstrated that SDF-1 promotes EMT in renal tubular epithelial cells with the involvement of the Wnt signaling pathway.

SDF-1/CXCR4 has been reported to serve an important role in the progression of EMT in different types of cells (13,17,27). AMD3100 is a synthetic blocker that inhibits the binding of SDF-1 to CXCR4. The Wnt pathway has been widely reported to be associated with fibrosis in different types of tissues (16,28). β-catenin is the most potent member of the downstream Wnt pathway. Activation of the Wnt pathway triggers intracellular signaling cascades by recruiting segment polarity protein dishevelled homolog DVL-1 (DVL-1) to the glycogen synthase kinase 3β complex, which protects β-catenin from proteasomal degradation (29). Subsequently, β-catenin accumulates in the cytoplasm and translocates into the nucleus, where it stimulates the expression of numerous genes that are involved in EMT (30). Hu *et al* (17) demonstrated that SDF-1/CXCR4 and the Wnt/β-catenin pathway have a synergistic effect in the EMT of colorectal cancer cells via downregulation of E-cadherin. E-cadherin, an exclusively expressed epithelial marker, may bind to the cytoplasmic domain of β-catenin and prevent its nuclear accumulation (31). In the present study, EMT was observed in renal tubular epithelial cells treated with SDF-1 through upregulation of α-SMA and downregulation of E-cadherin, and it was inhibited by AMD3100. Hu *et al* (17) also demonstrated that DKK-1 abolishes EMT by suppressing activation of the Wnt pathway. In the present study, EMT was also inhibited by DKK-1, and the Wnt pathway was demonstrated to be inactivated. Therefore, SDF-1 induces EMT in renal tubular epithelial cells *in vitro*, and the Wnt pathway may be one of the mechanisms involved.

The microarray in the present study revealed the association between CXXC5 mRNA and three lncRNAs. Previous studies have reported that CXXC5 is a negative regulator of the Wnt/β-catenin pathway (32,33) and that it interacts with DVL-1 (34-36). In the present study, a negative association between CXXC5 and the Wnt pathway was also observed in SDF-1-induced EMT. Notably, CXXC5 was downregulated in the cells treated with SDF-1 and DKK-1, and the three lncRNAs were upregulated. These data suggested that CXXC5 and the three lncRNAs may be downstream of SDF-1/CXCR4 and regulate activation of the Wnt pathway. Therefore, the present study may provide novel targets for investigating the detailed mechanisms of CAN and kidney fibrosis.

It is notable that the results of the present study do not entirely explain kidney allograft fibrosis, and the exact function of CXXC5 remains unknown. However, this study offers a novel insight into the progression of CAN and may also aid tumor research.

In conclusion, SDF-1 induces EMT by activating the Wnt/β-catenin pathway in NRK-52E cells, and this involves
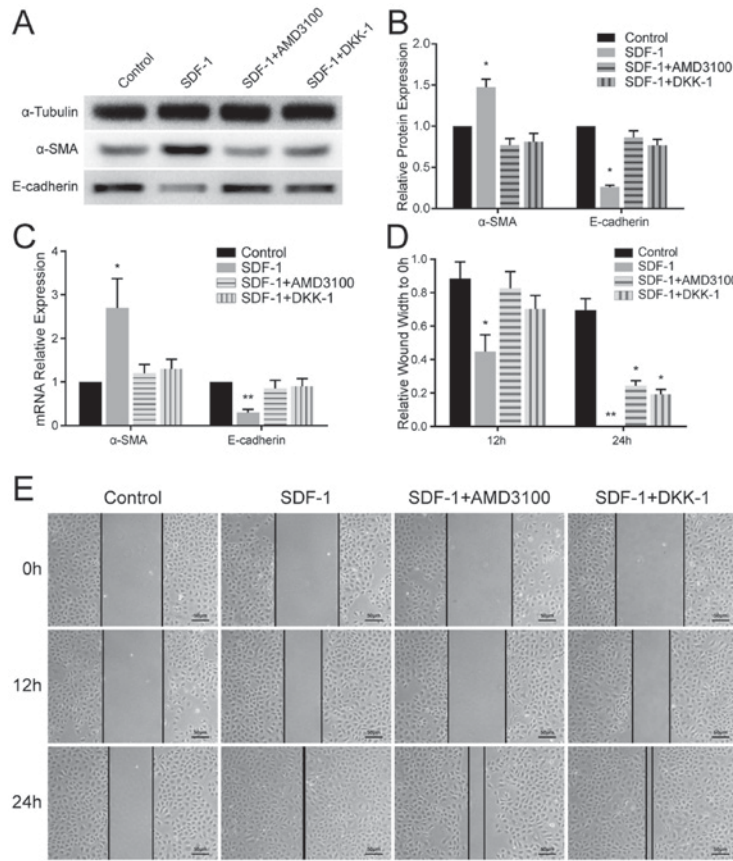
Figure 3. Epithelial-mesenchymal transition is induced by SDF-1 and inhibited by AMD3100 and DKK-1 *in vitro*. (A) WB demonstrated that the expression levels of α-SMA were increased and those of E-cadherin were reduced in the SDF-1 group, and these alterations were inhibited by AMD3100 and DKK-1, respectively. (B) Grayscale analysis of the WB. (C) Reverse transcription-quantitative polymerase chain reaction analysis revealed that the mRNA expression levels of α-SMA and E-cadherin corresponded to the results of the WB. (D) Quantitative analysis of the wound healing assay. (E) Representative images of the wound healing assay of the cells in the different groups at 0, 12 and 24 h post-scratching. $^*P<0.05$ and $^{**}P<0.01$ vs. control. SDF-1, stromal cell-derived factor 1; WB, western blotting.
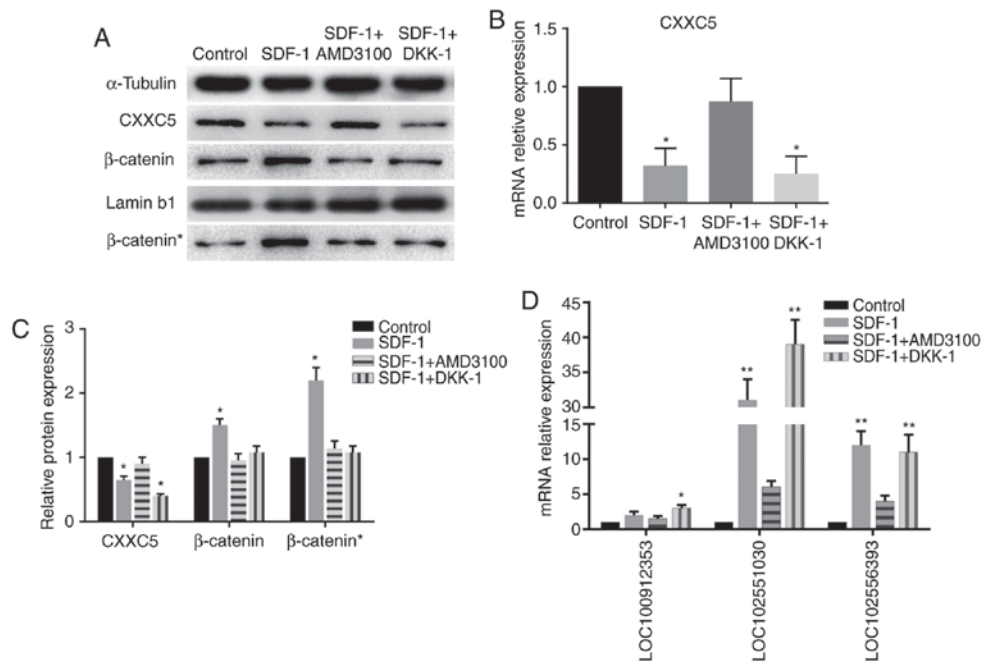

Figure 4. Markers of the Wnt/β-catenin pathway and associated long noncoding RNAs. (A) WB revealed that the expression of CXXC5 was downregulated in the SDF-1 group and the SDF-1 + DKK-1 group compared to the other two groups. The expression of both total β-catenin in the cells and nuclear β-catenin (β-catenin*) was upregulated in the SDF-1 group compared to the other three groups. (B) RT-qPCR demonstrated that CXXC5 mRNA was downregulated in the SDF-1 group and the SDF-1 + DKK-1 group. (C) The results of the grayscale analysis of the WB. (D) RT-qPCR revealed that the lncRNAs LOC100912353, LOC102551030 and LOC102556393 were upregulated. $^*P<0.05$ and $^{**}P<0.01$ vs. control. WB, western blotting; CXXC5, CXXC finger protein 5; SDF-1, stromal cell-derived factor 1; RT-qPCR, reverse transcription-quantitative polymerase chain reaction.

CXXC5 and three lncRNAs, which may be a novel mechanism and therapeutic target in CAN.

Availability of data and materials

The microarray data are available in the GEO database (GSE114088), and other data are included in this published article.

Authors' contributions

HT and YX contributed equally to this work, performed the microarray, WB and RT-qPCR, and were major contributors in writing the manuscript. ZZ performed the kidney transplantation in the rats. SZ performed the histological examination in the kidneys. WD and WJ assisted with analyzing the experimental results. XH provided the idea of this study. All authors read and approved the final manuscript.

Ethics approval and consent to participate

The animal protocols were approved by the Medical Research Center, Beijing Chaoyang Hospital, Capital Medical University (Beijing, China).

Patient consent for publication

Not applicable.

Competing interests

The authors declare they have no competing interests.

References

1. Lamb KE, Lodhi S and Meier-Kriesche HU: Long-term renal allograft survival in the United States: A critical reappraisal. Am J Transplant 11: 450-462, 2011.
2. Gatault P, Bertrand D, Büchler M, Colosio C, Hurault de Ligny B, Weestel PF, Rerolle JP, Thierry A, Sayegh J, Moulin B, *et al*: Eight-year results of the Spiesser study, a randomized trial comparing de novo sirolimus and cyclosporine in renal transplantation. Transpl Int 29: 41-50, 2016.
3. Solez K, Colvin RB, Racusen LC, Sis B, Halloran PF, Birk PE, Campbell PM, Cascalho M, Collins AB, Demetris AJ, *et al*: Banff '05 Meeting Report: Differential diagnosis of chronic allograft injury and elimination of chronic allograft nephropathy ('CAN'). Am J Transplant 7: 518-526, 2007.
4. Hara S: Banff 2013 update: Pearls and pitfalls in transplant renal pathology. Nephrology (Carlton) 20 (Suppl): S2-S8, 2015.
5. Mannon RB: Therapeutic targets in the treatment of allograft fibrosis. Am J Transplant 6: 867-875, 2006.
6. Takabatake Y, Sugiyama T, Kohara h, Matsusaka T, Kurihara H, Koni PA, Nagasawa Y, Hamano T, Matsui I, Kawada N, *et al*: The CXCL12 (SDF-1)/CXCR4 axis is essential for the development of renal vasculature. J Am Soc Nephrol 20: 1714-1723, 2009.
7. Ge G, Zhang H, Li R and Liu H: The function of SDF-1-CXCR4 axis in SP cells-mediated protective role for renal ischemia/reperfusion injury by SHH/GLI1-ABCG2 pathway. Shock 47: 251-259, 2017.
8. Xu Y, Zhang Q, Xue W, Zeng S, Zhang Z, Zhang X and Hu X: CXC chemokine receptor 4 (CXCR4) antagonist, a novel pathway to prevent chronic allograft nephropathy. Ann Transplant 21: 728-734, 2016.
9. Hu X, Okabayashi T, Cameron AM, Wang Y, Hisada M, Li J, Raccusen LC, Zheng Q, Montgomery RA, Williams GM and Sun Z: Chimeric allografts induced by short-term treatment with stem cell-mobilizing agents result in long-term kidney transplant survival without immunosuppression: A study in rats. Am J Transplant 16: 2055-2065, 2016.
10. Cameron AM, Wesson RN, Ahmadi AR, Singer AL, Hu X, Okabayashi T, Wang Y, Shigoka M, Fu Y, Gao W, *et al*: Chimeric allografts induced by short-term treatment with stem cell mobilizing agents result in long-term kidney transplant survival without immunosuppression: II, study in miniature swine. Am J Transplant 16: 2066-2076, 2016.
11. Zou XF, Gu JH, Cui ZL, Lu YW and Gu C: CXC chemokine receptor type 4 antagonism ameliorated allograft fibrosis in rat kidney transplant model. Exp Clin Transplant 15: 448-452, 2017.
12. Aversa I, Zolea F, Ieranò C, Bulotta S, Trotta AM, Faniello MC, De Marco C, Malanga D, Biamonte F, Viglietto G, *et al*: Epithelial-to-mesenchymal transition in FHC-silenced cells: The role of CXCR4/CXCL12 axis. J Exp Clin Cancer Res 36: 104, 2017.
13. He G, Ma M, Yang W, Wang H, Zhang Y and Gao MQ: SDF-1 in mammary fibroblasts of bovine with mastitis induces EMT and inflammatory response of epithelial cells. Int J Biol Sci 13: 604-614, 2017.
14. Wu CH, Song JS, Chang KH, Jan JJ, Chen CT, Chou MC, Yeh KC, Wong YC, Tseng CT, Wu SH, *et al*: Stem cell mobilizers targeting chemokine receptor CXCR4: Renoprotective application in acute kidney injury. J Med Chem 58: 2315-2325, 2015.
15. Yuan A, Lee Y, Choi U, Moeckel G and Karihaloo A: Chemokine receptor Cxcr4 contributes to kidney fibrosis via multiple effectors. Am J Physiol Renal Physiol 308: F459-F472, 2015.
16. von Toerne C, Schmidt C, Adams J, Kiss E, Bedke J, Porubsky S, Gretz N, Lindenmeyer MT, Cohen CD, Gröne HJ and Nelson PJ: Wnt pathway regulation in chronic renal allograft damage. Am J Transplant 9: 2223-2239, 2009.
17. Hu TH, Yao Y, Yu S, Han LL, Wang WJ, Guo H, Tian T, Ruan ZP, Kang XM, Wang J, *et al*: SDF-1/CXCR4 promotes epithelial-mesenchymal transition and progression of colorectal cancer by activation of the Wnt/beta-catenin signaling pathway. Cancer Lett 354: 417-426, 2014.
18. Shan S, Lv Q, Zhao Y, Liu C, Sun Y, Xi K, Xiao J and Li C: Wnt/beta-catenin pathway is required for epithelial to mesenchymal transition in CXCL12 over expressed breast cancer cells. Int J Clin Exp Pathol 8: 12357-12367, 2015.
19. Council NR: Guide for the care and use of laboratory animals: Eighth edition. The National Academies Press, Washington, DC, 2011.
20. Kahu J, Kyllonen L, Raisanen-Sokolowski A and Salmela K: Donor risk score and baseline biopsy CADI value predict kidney graft outcome. Clin Transplant 25: E276-E283, 2011.
21. Livak KJ and Schmittgen TD: Analysis of relative gene expression data using real-time quantitative PCR and the 2(-Delta Delta C(T)) method. Methods 25: 402-408, 2001.
22. Shi J, Li F, Luo M, Wei J and Liu X: Distinct roles of Wnt/beta-catenin signaling in the pathogenesis of chronic obstructive pulmonary disease and idiopathic pulmonary fibrosis. Mediators Inflamm 2017: 3520581, 2017.
23. Sanchez-Duffhues G, Garcia de Vinuesa A and Ten Dijke P: Endothelial-to-mesenchymal transition in cardiovascular diseases: Developmental signaling pathways gone awry. Dev Dyn 247: 492-508, 2018.
24. Lin MF, Jungreis I and Kellis M: PhyloCSF: A comparative genomics method to distinguish protein coding and non-coding regions. Bioinformatics 27: i275-i282, 2011.
25. Sun X, Cheng G, Hao M, Zheng J, Zhou X, Zhang J, Taichman RS, Pienta KJ and Wang J: CXCL12/CXCR4/CXCR7 chemokine axis and cancer progression. Cancer Metastasis Rev 29: 709-722, 2010.
26. Zuk A, Gershenovich M, Ivanova Y, MacFarland RT, Fricker SP and Ledbetter S: CXCR(4)antagonism as a therapeutic approach to prevent acute kidney injury. Am J Physiol Renal Physiol 307: F783-F797, 2014.

27. Xia R, Xu G, Huang Y, Sheng X, Xu X and Lu H: Hesperidin suppresses the migration and invasion of non-small cell lung cancer cells by inhibiting the SDF-1/CXCR-4 pathway. Life Sci 201: 111-120, 2018.
28. Tao h, Yang JJ, Shi KH and Li J: Wnt signaling pathway in cardiac fibrosis: New insights and directions. Metabolism 65: 30-40, 2016.
29. Luo K, Gu X, Liu J, Zeng G, Peng L, Huang H, Jiang M, Yang P, Li M, Yang Y, et al: Inhibition of disheveled-2 resensitizes cisplatin-resistant lung cancer cells through down-regulating Wnt/beta-catenin signaling. Exp Cell Res 347: 105-113, 2016.
30. Gilles C, Polette M, Mestdagt M, Nawrocki-Raby B, Ruggeri P, Birembaut P and Foidart JM: Transactivation of vimentin by beta-catenin in human breast cancer cells. Cancer Res 63: 2658-2664, 2003.
31. Wong SHM, Fang CM, Chuah LH, Leong CO and Ngai SC: E-cadherin: Its dysregulation in carcinogenesis and clinical implications. Crit Rev Oncol Hematol 121: 11-22, 2018.
32. Andersson T, Sodersten E, Duckworth JK, Cascante A, Fritz N, Sacchetti P, Cervenka I, Bryja V and Hermanson O: CXXC5 is a novel BMP4-regulated modulator of Wnt signaling in neural stem cells. J Biol Chem 284: 3672-3681, 2009.
33. Kim HY, Yoon JY, Yun JH, Cho KW, Lee SH, Rhee YM, Jung HS, Lim HJ, Lee H, Choi J, et al: CXXC5 is a negative-feedback regulator of the Wnt/beta-catenin pathway involved in osteoblast differentiation. Cell Death Differ 22: 912-920, 2015.
34. Lee SH, Kim MY, Kim HY, Lee YM, Kim H, Nam KA, Roh MR, Min Do S, Chung KY and Choi KY: The dishevelled-binding protein CXXC5 negatively regulates cutaneous wound healing. J Exp Med 212: 1061-1080, 2015.
35. Lee SH, Seo SH, Lee DH, Pi LQ, Lee WS and Choi KY: Targeting of CXXC5 by a competing peptide stimulates hair regrowth and wound-induced hair neogenesis. J Invest Dermatol 137: 2260-2269, 2017.
36. Ma S, Choi J, Jin X, Kim HY, Yun JH, Lee W, Choi KY and No KT: Discovery of a small-molecule inhibitor of Dvl-CXXC5 interaction by computational approaches. J Comput Aided Mol Des 32: 643-655, 2018.